Carbohydrate Polymers 324 (2024) 121517

Contents lists available at ScienceDirect

Carbohydrate Polymers

journal homepage: www.elsevier.com/locate/carbpol

Towards the semi-synthesis of phosphorylated mimics of glycosaminoglycans: Screening of methods for the regioselective phosphorylation of chondroitin

Fabiana Esposito, Serena Traboni, Alfonso Iadonisi, Emiliano Bedini *

Department of Chemical Sciences, University of Naples Federico II, Complesso Universitario Monte S.Angelo, via Cintia 4, I-80126 Napoli, Italy

ARTICLE INFO

Keywords:
Glycosaminoglycans
Chondroitin
Phosphorylation
Sulfated GAG mimics
NMR spectroscopy
Biomimetic reaction

ABSTRACT

Glycosaminoglycan (GAG) mimics carrying phosphate rather than sulfate anionic groups have been poorly investigated, in spite of their interesting perspectives. While some GAG-mimicking phosphorylated polymers have been reported, to the best of our knowledge no phosphorylated polysaccharides having the same backbone of natural sulfated GAGs have been accessed yet. To fill this gap, in this work two standard phosphorylation protocols and two recently reported procedures have been screened on a set of polysaccharide species composed by microbial sourced chondroitin and three partially protected, semi-synthetic derivatives thereof. A detailed structural characterization by ^{1}H, ^{13}C and ^{31}P NMR spectroscopy revealed the higher versatility of the innovative, biomimetic reaction employing monopotassium salt of phosphoenolpyruvate (PEP—K) with respect to standard phosphorylating agents (phosphoric acid or phosphorus oxychloride). Indeed, PEP-K and H_3PO_4 gave similar results in the regioselective phosphorylation of the primary hydroxyls of unprotected chondroitin, while only the former reacted on partially protected chondroitin derivatives in a controlled, regioselective fashion, affording chondroitin phosphate (CP) polysaccharides with different derivatization patterns. The reported results represent the first, key steps towards the systematic semi-synthesis of phosphorylated GAGs as a new class of GAG mimics and to the evaluation of their biological activities in comparison with native sulfated GAGs.

1. Introduction

Sulfated glycosaminoglycans (GAGs) are a family of complex polysaccharides largely distributed in the animal kingdom, in particular in mammals. They are highly negatively charged, linear biomacromolecules, composed of alternating aminosugar and uronic acid (or neutral hexose) monomers organized in disaccharide repeating units, that are extensively decorated with sulfate groups. GAG sulfation is a dynamic and complex post-translational modification process that is orchestrated by enzymes called sulfotransferases. It seems to be a result of evolution allowing sulfated GAGs to play key roles in several physiological and pathological processes typical of higher animals (*e.g.* central nervous system development, stem cell differentiation, cancer cell progression *etc.*) (Soares da Costa et al., 2017). The diverse bioactivities of sulfated GAGs allowed their application as therapeutics for the treatment of several diseases. Nonetheless, the medical use of native sulfated GAGs is made difficult by several factors (Pomin, 2015): i) the low yields, high costs and complex protocols for their isolation; ii) the animal sources raising ethical and sustainability concerns as well as strict regulatory issues; iii) the risk of contaminations (Restaino et al., 2017) in particular with harmful compounds (Guerrini et al., 2008); iv) their significant structural heterogeneity in terms of sulfate groups distribution along the GAG polysaccharide chain, that depends not only on animal species and tissue but also on the physio-pathological conditions of the individual animal (Collin et al., 2017; Han et al., 2020), thus hampering a precise control of the sulfation pattern. These drawbacks have fueled researchers' efforts to open an access to sulfated GAGs species from non-animal sources. To this aim, diverse approaches have been reported (Perez et al., 2023): total synthesis by chemical (Mende et al., 2016) or (chemo-)enzymatic strategies (Gottschalk & Elling, 2021; Zhang et al., 2020); production by microbial cell factories (Badri et al., 2021) and combined microbiological-chemical strategies (Bedini et al., 2011). Furthermore, the production of sulfated GAG mimics and analogues has been also tackled (Afosah & Al-Rohani, 2020; Liu et al., 2019) and currently represents an interesting research field. Indeed, some sulfated GAG mimics are able not only to imitate structures and

* Corresponding author.
E-mail address: ebedini@unina.it (E. Bedini).

https://doi.org/10.1016/j.carbpol.2023.121517
Received 19 May 2023; Received in revised form 3 October 2023; Accepted 18 October 2023
Available online 20 October 2023

bioactivities of naturally occurring sulfated GAGs but also to improve the pharmacological properties of the latter and enlarge the therapeutic applications. In this frame, different kinds of compounds have been obtained: i) sulfated non-GAG polysaccharides produced by chemical sulfation of common polysaccharides from non-animal sources (plants, algae, microbia) (Arlov et al., 2021; Zeng et al., 2019); ii) sulfated non-GAG oligosaccharides accessed by total synthesis (Tyrikos-Ergas et al., 2022); iii) synthetic, sulfated non-saccharide mimics with oligomeric (Alfieri et al., 2021; Morla et al., 2023) or polymeric (Nie et al., 2021) structures. Conversely, analogues displaying negative charges on groups different from sulfates are still underdeveloped (Bojarski et al., 2019; Khaybrakhmanova et al., 2022), in spite of their interesting perspectives. For example, by replacing the sulfate groups of GAGs with phosphates, their differences in size, polarity, acid-base and chelation properties could lend unreported activities to phosphorylated GAGs, as indicated by a recent *in silico* study comparing the structural flexibility and intra- and intermolecular interaction patterns of native chondroitin sulfate (CS) and hyaluronic acid (HA) with their phosphorylated counterparts (Bojarski et al., 2019). Indeed, this theoretical investigation suggested that phosphorylated GAGs could bind proteins generally with a stronger affinity than their sulfated counterparts and the differences in the binding modes might be highly dependent on the protein target. This would propose phosphorylated GAGs as promising, new species to specifically control biochemical processes where the mediating role of sulfated GAGs is crucial.

Some GAG-mimicking phosphorylated polymers have been very recently reported (Varghese et al., 2022), whereas – to the best of our knowledge – a (semi)-synthetic access to phosphorylated species having the same polysaccharide backbone of natural sulfated GAGs is still lacking. The introduction of phosphate groups on polysaccharide backbones currently presents several concerns: i) the rather harsh conditions required by the commonly employed methods (*e.g.* phosphoric acid and urea at temperatures up to 160 °C), ii) the low degrees of derivatization that are generally achieved on common polysaccharides such as cellulose, dextran, alginate, (Illy et al., 2015; Laffargue et al., 2023; Wang et al., 2022; Zhou & Huang, 2021); iii) the much lower number of publications reporting a control of the regiochemistry in phosphate groups installation on polysaccharides with respect to their regioselective sulfation (Bedini et al., 2017).

The regioselective derivatization of polysaccharides can be generally tackled either by looking for direct reactions enabling the targeted, regioselective structural modification or by designing a proper multistep strategy based on the regioselective installation and cleavage of suitable protecting groups. While few, scattered reports can be found in literature exploiting the former approach for the regioselective phosphorylation of polysaccharides (Coleman et al., 2011; Niu et al., 2013; Schmieder et al., 2013), to the best of our knowledge no regiocontrolled phosphate group installation through the latter strategy has been published yet, in spite of a potential, much higher versatility in terms of range of targetable derivatives. Actually, this gap is mainly dictated by the harsh reaction conditions required by standard polysaccharide phosphorylation methods (Illy et al., 2015), that are scarcely compatible with protecting groups employment.

Very recently, a number of innovative methods for the (poly)-phosphorylation of complex biomolecules such as peptides, carbohydrates, oligonucleotides and secondary metabolites appeared in literature (Domon et al., 2020; Lin et al., 2022; Ociepa et al., 2021). They share a high chemoselectivity and the unprecedented employment of P(V) phosphorylating agents much milder than H_3PO_4, $POCl_3$ and derivatives. Furthermore, they are more biomimetic than the classical phosphoramidite-type P(III) reagents (Knouse et al., 2021). With the aim to fill the lack of an access to regioselectively phosphorylated GAG polysaccharides, in this work two of these novel methods (Domon et al., 2020; Ociepa et al., 2021) have been tested and compared to H_3PO_4- and $POCl_3$-based standard procedures. The chosen substrate has been an unsulfated chondroitin (CS-0) polysaccharide deriving from the fed-batch fermentation of *Escherichia coli* O5:K4:H4 (Cimini et al., 2018), having a weight-averaged molecular weight M_w value of 47 ± 3 kDa (1.34 dispersity) and the same polysaccharide backbone of natural CSs from animal sources but without any sulfate group decoration on it (Cimini et al., 2023).

2. Experimental

2.1. General methods

E. coli-sourced CS-0 was a kind gift of Prof. C. Schiraldi (Department of Experimental Medicine, Università della Campania "L.Vanvitelli"). Commercial grade reagents and solvents were purchased from Thermo Fisher Scientific but (2*S*,3a*S*,6*R*,7a*S*)- -methyl-2-((4-bromophenyl)thio)-6-(prop-2-yl)hexahydrobenzo[d][1,3,2]oxathiaphosphole 2-oxide (Ψ^0) from Merck, and used without further purification, except where differently indicated. Dialyses were conducted on Spectra/Por 3.5 kDa cut-off membranes at 4 °C. Centrifugations were performed with an Eppendorf Centrifuge 5804R instrument at 4 °C (4600 g, 5 min). Freeze-dryings were performed with a 5Pascal Lio 5P 4 K freeze dryer. Elemental analysis was performed with a ThermoFischer FlashSmart V CHNS instrument. NMR spectra were recorded on a Bruker Avance-III HD (^{1}H: 400 MHz, ^{13}C: 100 MHz, ^{31}P: 162 MHz) or on a Bruker Avance-III (^{1}H: 600 MHz, ^{13}C: 150 MHz) instrument – the latter equipped with a cryo-probe – in D_2O (acetone as internal standard, ^{1}H: $(CH_3)_2CO$ at δ 2.22; ^{13}C:$(CH_3)_2CO$ at δ 31.5; H_3PO_4 as external standard, ^{31}P: δ 0.0). Data were processed using the data analysis packages integrated with Bruker TopSpin® 4.0.5 software. ^{1}H-DOSY experiments were measured with a diffusion time of 100 ms. ^{31}P NMR spectra were obtained by typically accumulating 512 transients. Gradient-selected COSY and TOCSY experiments were performed using spectral widths of either 6000 Hz in both dimensions, using data sets of 2048 × 256 points. ^{1}H,^{13}C-HSQC, ^{1}H,^{13}C-HSQC-TOCSY and ^{1}H,^{13}C-HMBC experiments were measured in the ^{1}H-detected mode *via* single quantum coherence with proton decoupling in the ^{13}C domain, using data sets of 2048 × 256 points and typically 80 increments (160 for HMBC). ^{1}H,^{31}P-HMBC experiments were measured in the ^{1}H-detected mode *via* a phase sensitive gradient selection with decoupling during acquisition, using data set of 2048 × 256 points and typically 100 increments. ^{31}P-DOSY were measured with a 2D sequence using bipolar gradient pulses with a diffusion time of 50 ms, acquiring data sets of 4096 × 64 points and typically 128 increments.

2.2. Typical procedure for phosphorylation with H_3PO_4

A mixture of chondroitin *n*-tetrabutylammonium salt 4 (99.0 mg, 0.159 mmol) and urea (1.48 g, 24.6 mmol) was dried under vacuum, purged under argon, then treated with dry DMF (3.0 mL) and heated to 100 °C. The resulting solution was treated with a 85 % solution of H_3PO_4 in water (257 μL). The mixture was stirred at 120 °C (150 °C for reactions on 1–3) for 3 h. The obtained yellowish suspension was then cooled to room temperature and methanol (30 mL) was added to form a white precipitate. The mixture was cooled in freezer for 1 h, then the precipitate was collected by centrifugation. The solid was dissolved in HPLC-grade H_2O (6.0 mL; pH ~ 2) and treated with a few drops of a 33 % solution of NaOH in water to neutral pH (for reactions on 1–3, a pH ≥ 12 was reached and the alkaline solution was stirred at rt. overnight and then neutralized with a 1 M solution of HCl in water; for reaction on 3, additional 2 h stirring at 50 °C was performed before NaOH addition). After dialysis and freeze-drying, phosphorylated product CP-i was obtained (73.4 mg, 74 % mass yield). An aliquot (9.9 mg) was further purified by size-esclusion chromatography (6.8 mg purified product recovered).

2.3. Typical procedure for phosphorylation with $POCl_3$

A 41.2 mM solution of 4 (56.4 mg, 90.6 μmol) in dry DMF (2.2 mL) was treated with a freshly prepared 9:1 *v*/v pyridine-$POCl_3$ mixture (2.2 mL). After overnight stirring at rt., the resulting brownish mixture was diluted with a 33 % solution of NaOH in water and stirred for 1 h (overnight for reactions on 1–3). Dialysis and freeze-drying afforded CP-ii (36.2 mg, 64 % mass yield). In the case of reaction on 3, the product was further treated with a 1 M solution of HCl in water (pH ~ 2), stirred at 50 °C for 2 h, then neutralized with a 33 % solution of NaOH in water, dialyzed and freeze-dried.

2.4. Typical procedure for phosphorylation with PEP—K

Compound 4 (127 mg, 0.204 mmol) was mixed with *n*-tetrabutylammonium bisulfate (TBAHS, 41.4 mg, 0.122 mmol) and the monopotassium salt of phosphoenolpyruvate (PEP—K, 421 mg, 2.04 mmol). Dry DMF (5.6 mL) was then added under argon atmosphere. The resulting suspension was stirred at 80 °C (or 100 °C: see Table 1) for 48 h, then cooled to rt. and treated with acetone saturated with NaCl (7 mL) to form a yellowish precipitate. The mixture was cooled in freezer for 1 h, then the precipitate was collected by centrifugation, and subsequently dissolved in HPLC-grade H_2O (10 mL). The solution was neutralized with a few drops of a 33 % solution of NaOH in water (for reactions on 1–3, a pH ≥ 12 was reached and the alkaline solution was stirred at rt. overnight and then neutralized with a 1 M solution of HCl in water; for reaction on 3, additional 2 h stirring at 50 °C was performed before NaOH addition). After dialysis and freeze-drying, phosphorylated product CP-iii was obtained (123 mg, 97 % mass yield). An aliquot (18.8 mg) was further purified by size-esclusion chromatography (stationary phase = Sephadex G-10 dextran; column volume = 250 cm^3; mobile phase = double-distilled water; flow rate = 0.24 mL/min; fraction size = 1.5 mL; detector = Knauer K-2310 refractive index refractometer; 11.7 mg purified product recovered).

Table 1
Phosphorylation tests on chondroitin substrates 1–4.

Entry	Product	Substrate	Phosphorylation conditions[a]	Phosphorylation position (DP)
1	CP-i	4	H_3PO_4, urea, 120 °C, 3 h	GalNAc *O*-6 (49 %)
2	CP-ii	4	$POCl_3$, pyridine, rt., 18 h	–[b]
3	CP-iii	4	Ψ^O, DBU, rt., 1 h	–[b]
4	CP-iv	4	PEP-K (10 eqs), TBAHS (0.6 eqs), 80 °C, 48 h	GalNAc *O*-6 (36 %)
5	CP-v	2	H_3PO_4, urea, 150 °C, 3 h	n.d.[c]
6	CP-vi	2	$POCl_3$, pyridine, rt., 18 h	n.d.[c]
7	CP-vii	2	Ψ^O, DBU, rt., 1 h	–[b]
8	CP-viii	2	PEP-K (10 eqs), TBAHS (0.6 eqs), 80 °C, 48 h	–
9	CP-ix	2	PEP-K (30 eqs), TBAHS (1.2 eqs), 100 °C, 48 h	–
10	CP-x	2	PEP-K (50 eqs), TBAHS (2.0 eqs), 80 °C, 24 h	GalNAc *N*-2 (29 %)
11	CP-xi	2	PEP-K (50 eqs), TBAHS (2.0 eqs), 100 °C, 48 h	GalNAc *N*-2 (10 %)
12	CP-xii	1	H_3PO_4, urea, 150 °C, 3 h	n.d.[c]
13	CP-xiii	1	$POCl_3$, pyridine, rt., 18 h	n.d.[c]
14	CP-xiv	1	PEP-K (50 eqs), TBAHS (2.0 eqs), 100 °C, 48 h	GalNAc *O*-6 (80 %)
15	CP-xv	3	H_3PO_4, urea, 150 °C, 3 h	n.d.[c]
16	CP-xvi	3	$POCl_3$, pyridine, rt., 18 h	n.d.[c]
17	CP-xvii	3	Ψ^O, DBU, rt., 1 h	–
18	CP-xviii	3	PEP-K (50 eqs), TBAHS (2.0 eqs), 100 °C, 48 h	GlcA *O*-2 (19 %) GalNAc *O*-6 (4 %)

[a] Reactions were all conducted in dry DMF.
[b] Attempted twice (see Figs. S24-S26 in Supporting Information).
[c] Not determined.

2.5. Typical procedure for phosphorylation with Ψ^O

A mixture of compound 4 (21.3 mg, 32.7 μmol) and Ψ^0 (43.8 mg, 98.1 μmol) was suspended in dry DMF (1.2 mL) under Ar atmosphere. A freshly prepared 1.68 mM solution of 1,8-diazabicyclo[5.4.0]undec-7-ene (DBU) in dry DMF (58.5 μL, 98.5 μmol) was then added and the resulting mixture was stirred at rt. for 1 h. Thereafter, double-distilled water (2.5 mL) and then some drops of a 1 M solution of NaOH in water (till pH > 10) were added. After overnight stirring at rt., the resulting precipitate was collected by centrifugation and discarded, while the supernatant was dialyzed and then freeze-dried to afford product CP-iii (23.1 mg, 108 % mass yield).

2.6. Elemental analysis and degree of sulfation

Elemental analysis was performed using a FlashSmart V CHNS instrument (ThermoFischer) with sulfanilamide as standard, to determine the mean carbon (%C) and sulfur (%S) contents of sample CP-xiv. The degree of sulfation (DS) was calculated using mean %C and %S values following the Eq. (1):

$$DS = \frac{\%S}{\%C} \times \frac{awC}{awS} \times nC \quad (1)$$

where awC and awS are the atomic weights of carbon (C) and sulfur (S), respectively, and nC is the number of carbon atoms (14) per disaccharide repeating units.

3. Results and discussion

3.1. Preparation of chondroitin substrates

The first part of the work was dedicated to the preparation of a set of CS-0 derivatives, having a different pattern of protecting groups distributed within the disaccharide repeating unit, that is composed of alternating 2-acetamido-2-deoxy-D-galactose (*N*-acetyl-galactosamine, GalNAc) and D-glucuronic acid (GlcA) residues. In particular, derivatives 1–3 were designed with protecting groups at every functional group of the disaccharide repeating unit but the hydroxyl at GalNAc-4,6 or GalNAc-4 or GlcA-2 position, respectively (Fig. 1). They might serve as proper substrates for the regioselective installation of phosphate groups at the positions of disaccharide repeating units, that are most commonly sulfated in natural CS polysaccharides (Volpi et al., 2021). Derivatives 1–3 were semi-synthesized from *E. coli*-sourced CS-0 through known multi-step procedures (Vessella, Marchetti, et al., 2021; Vessella, Traboni, Cimini, et al., 2019; Vessella, Traboni, Pirozzi, et al., 2019). Derivative 4, without any protecting group and having *n*-tetrabutylammonium as GlcA carboxylate counterion, was also prepared (Vessella, Vázquez, et al., 2021), in order to increase the solubility in organic solvents of the unprotected CS-0 polysaccharide, that could be tested for the regioselective phosphorylation at the most reactive site of its repeating unit, *i.e.* primary hydroxyl at GalNAc-6 position.

3.2. Screening of phosphorylation reactions

The screening of phosphorylation reactions started by subjecting derivative 4 to two standard protocols for polysaccharide phosphorylation, employing H_3PO_4 and urea in DMF at high temperatures (120–150 °C) or $POCl_3$ and pyridine in DMF at room temperature. The recently introduced biomimetic procedure for alcohol phosphorylation (Domon et al., 2020) using a combination of PEP-K and TBAHS in DMF at 80 °C, was also tested (Fig. 2). Furthermore, the screening included a phosphorylation procedure employing the chiral, limonene-derived reagent Ψ^O in combination with DBU as hindered base. This method has been very recently demonstrated to work efficiently on both simple and medicinally relevant alcohols (Ociepa et al., 2021). A treatment with

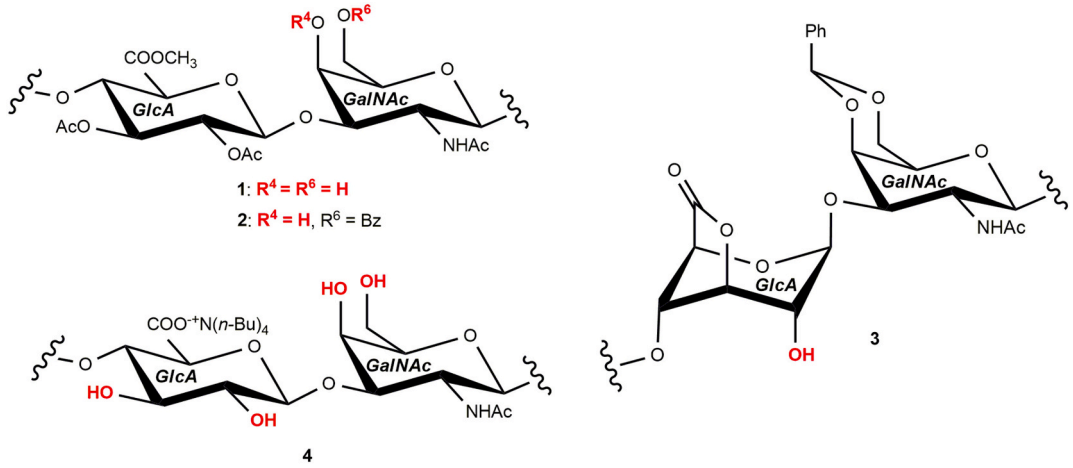

Fig. 1. CS-0 derivatives subjected to phosphorylation reaction screening.

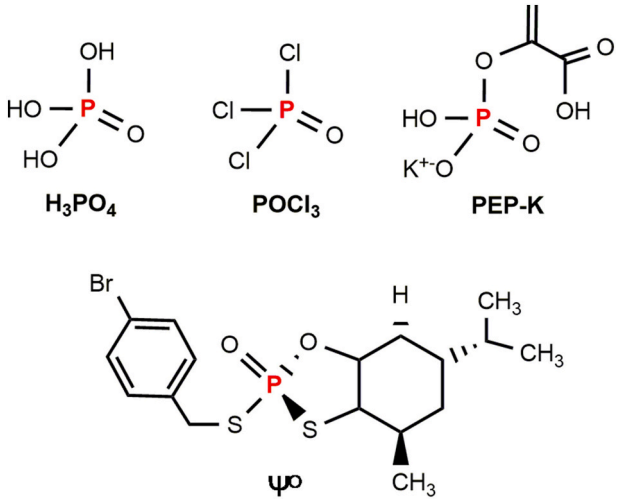

Fig. 2. Chemical structure of the phosphorylating reagents employed in this work.

aqueous NaOH followed the phosphorylation in all cases, in order to substitute GlcA carboxylate tetrabutylammonium counterion with Na^+. Finally, a sequential purification by dialysis and size-exclusion chromatography furnished products CP-i-iv (Table 1, entries 1–4). The four phosphorylation procedures described above were also tested on regioselectively protected chondroitin substrates 1–3 (Table 1, entries 5–18).

3.3. Structural characterization of phosphorylated chondroitin polysaccharides

The structures of the obtained phosphorylated chondroitin polysaccharides were investigated by 1D- and 2D-NMR techniques. A comparison of the ^{1}H NMR spectra measured on *E. coli*-sourced CS-0 starting material and the semi-synthetic phosphorylated polysaccharides was firstly performed. In the case of CP-i-iv derivatives obtained from the unprotected substrate 4, the ^{1}H NMR analysis revealed the presence of new signals at δ 3.87, 4.02 and 4.16 in CP-i,iv spectra (Fig. 3b-f and Table 2), while no clear differences between CS-0 and CP-ii or CP-iii samples could be found. In order to gain more insights into the structure of derivatives CP-i,iv, a set of ^{1}H,^{1}H-, ^{1}H,^{13}C- and ^{1}H,^{31}P-2D-NMR spectra were measured. The analysis of the ^{1}H,^{13}C-DEPT-HSQC 2D-NMR spectrum (Figs. 3g and S1 in Supporting Information) revealed the presence of two methylene signals, at $\delta_{H/C}$ 4.02/65.6 and 3.73–3.82/62.4. The former could be unambiguously assigned to the CH_2 group at position *O*-6 of 6-phosphorylated GalNAc (GalNAc6P) units by the main signal detected at $\delta_{H/P}$ 4.02/0.73 in the ^{1}H,^{31}P-HMBC 2D-NMR spectrum (Figs. 3i and S3 in Supporting Information), while the latter was due to unsubstituted GalNAc 6-*O*-CH_2 moieties as confirmed by comparison with CS-0 spectra (Figs. S2 and S4 in Supporting Information). A relative integration of the two methylene signals volumes in the ^{1}H,^{13}C-DEPT-HSQC spectrum of CP-i and CP-iv (by assuming that the signals displayed similar $^1J_{C,H}$ coupling constants and that a difference of around 5–8 Hz from the experimental set value could not cause a substantial variation of the integrated peak volumes (Guerrini et al., 2005)) returned a similar degree of phosphorylation (DP) for the two CP products (49 % and 36 % for CP-i and CP-iv, respectively). Apart the signal at δ 0.73, the ^{31}P NMR spectrum of CP-iv revealed also a marked peak at δ 0.28, that could be assigned by a ^{31}P-DOSY 2D-NMR spectrum (Fig. 3h) to residual, fast diffusing, inorganic phosphate, in agreement with literature reporting the difficulty in removing the latter quantitatively from phosphorylated polysaccharides (Lowman et al., 1998).

With respect to the polysaccharides derived by phosphorylation of substrate 2, standard protocols employing H_3PO_4 or $POCl_3$ (Table 1, entries 5,6) gave markedly heterogeneous products, as detected by ^{1}H NMR spectra, showing highly broadened signals (Fig. 4g-h). Conversely, some slight differences could be found between starting CS-0 and the CP-vii obtained by reaction of 2 with Ψ^O (Fig. 4f). Nonetheless, the absence of any significant peak in the ^{31}P NMR spectrum (Fig. S5 in Supporting Information) of the latter clearly demonstrated that no phosphate groups were appended on chondroitin backbone (Table 1, entry 7). Similarly, no differences were found between the ^{1}H NMR spectra of starting CS-0 and the product obtained with PEP-K (Fig. 4e) under the conditions successfully employed on 4 (entry 8). An increase of PEP-K and TBAHS amounts and of reaction temperature (entries 9–11) afforded CP derivatives showing ^{1}H NMR spectra with minor signals at δ 4.43 and 5.08, that could not be detected in the spectrum of *E. coli*-sourced CS-0 (Fig. 4b-d). CP-x and CP-xi derivatives showed these signals at much higher intensity with respect to CP-ix. Surprisingly, the ^{1}H,^{31}P-HMBC spectrum of CP-x revealed that none of these signals gave cross-peaks with ^{31}P signals (Fig. 4k). A set of ^{1}H,^{1}H- and ^{1}H,^{13}C-correlated spectra (COSY, TOCSY, DEPT-HSQC, HSQC-TOCSY and HMBC; Figs. S6 and S8 in Supporting Information) allowed the full assignment of ^{1}H and ^{13}C chemical shifts of CP-x ^{1}H,^{13}C-DEPT-HSQC spectrum (Fig. 4j and Table 2). In particular, the anomeric signal at $\delta_{H/C}$ 5.08/100.3 gave a HMBC correlation with the signal at $\delta_{H/C}$ 4.76/72.7, which could be assigned to the CH atoms at position 5 of an uronic acid moiety by HMBC correlation with a carboxyl signal at δ_C 176.6. COSY, TOCSY and HSQC-TOCSY 2D-NMR spectra allowed the assignment of chemical shifts also for the CH atoms at positions 2, 3 and 4 of the same residue (Table 2),

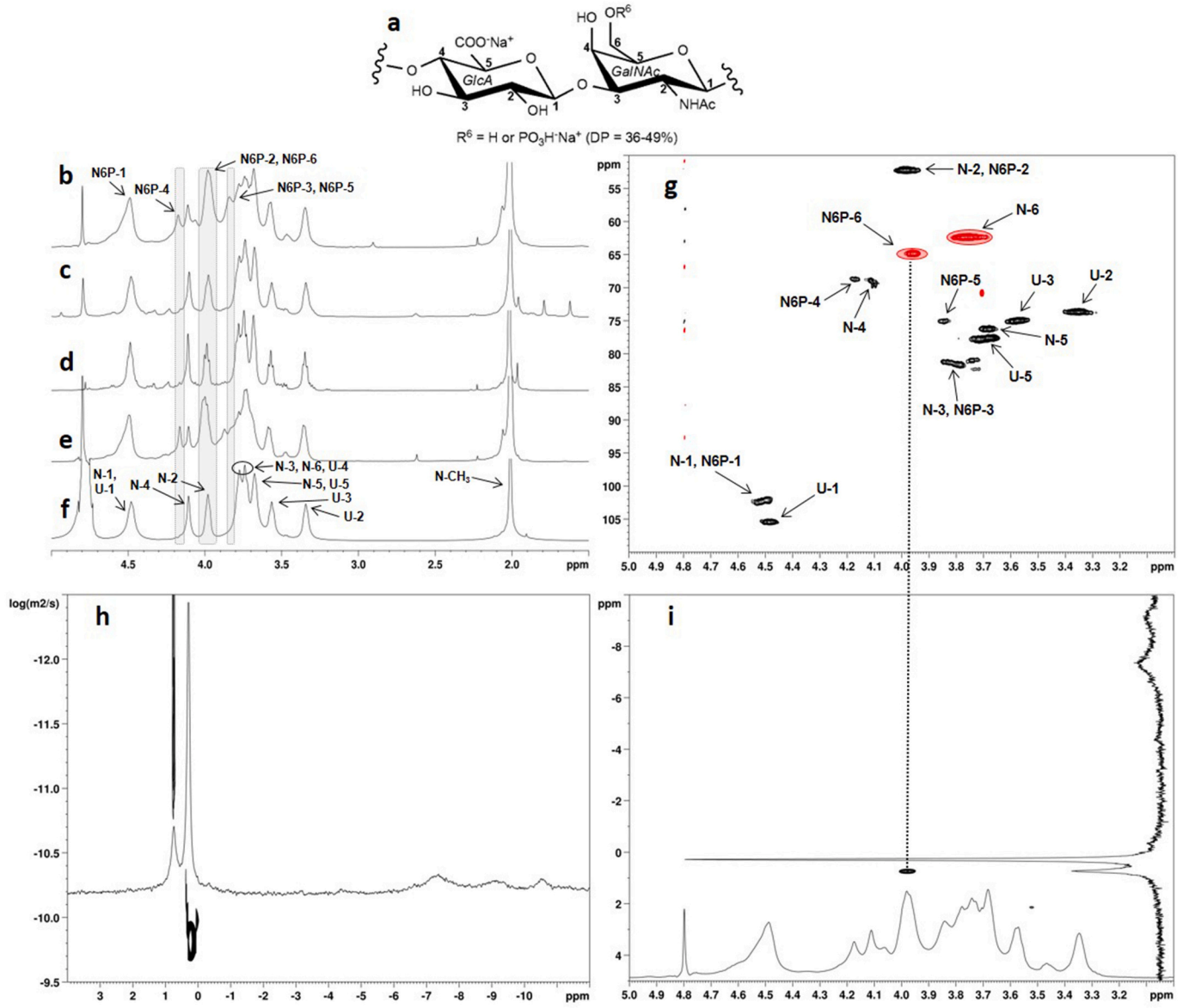

Fig. 3. (a) Structure of phosphorylated polysaccharides (CP-i and CP-iv; see Table 1 for details) semi-synthesized from derivative 4; (b-f) ^{1}H NMR spectra (600 MHz, 298 K, D_2O) of CP-iv (b), CP-iii (c), CP-ii (d), CP-i (e) and CS-0 (f) (N = GalNAc, N6P = GalNAc6P, U = GlcA; the grey stripes highlight the main differences among the spectra); (g) ^{1}H,^{13}C-DEPT-HSQC 2D-NMR spectra (600 MHz, 298 K, D_2O, zoom) of CP-iv (densities enclosed in red circles were integrated for DP estimation); (h) superimposed ^{31}P NMR and ^{31}P-DOSY 2D-NMR spectra (162 MHz, 298 K, D_2O, zoom) of CP-iv; (i) superimposed ^{1}H-, ^{31}P NMR and ^{1}H,^{31}P-HMBC 2D-NMR spectra (400 and 162 MHz, 298 K, D_2O) of CP-iv.

Table 2
^{1}H-, ^{13}C- (in italic) and ^{31}P NMR chemical shift values of major monosaccharide components of CP-iv, CP-x, CP-xiv and CP-xviii (see Figs. 3a, 4a and 5a for atoms numbering).

Residue	Derivative	1	2	3	4	5	6	Ac CH_3	^{31}P
GalNAc	CP-iv, CP-x,	4.50	3.99	3.79	4.11	3.69	3.73–3.82	2.01	–
	CP-xiv, CP-xviii	*102.1*	*52.2*	*81.6*	*69.0*	*76.3*	*62.4*	*23.8*	
GlcA	CP-iv, CP-x,	4.49	3.35	3.57	3.74	3.68	–	–	–
	CP-xiv, CP-xviii	*105.6*	*73.8*	*74.8*	*80.9*	*76.3*	*175.8*		
IdoA	CP-ix	5.08	3.77	4.01	4.43	4.76	–	–	–
		100.3	*69.5*	*70.1*	*79.2*	*72.7*	*176.6*		
GalNAc6P	CP-iv, CP-xiv,	4.53	3.99	3.83	4.16	3.87	4.02	2.06	0.73
	CP-xviii	*102.6*	*52.2*	*81.3*	*68.6*	*74.9*	*65.6*	*24.0*	
GalNAc4S6P	CP-xiv	4.59	4.07	3.86	4.76	3.78	3.99	2.02	1.43
		102.0	*52.1*	*75.2*	*77.1*	*68.6*	*65.2*	*23.8*	
GlcA2P	CP-xviii	4.58	3.82	3.71	3.86	3.75	–	–	0.19
		103.1	*77.4*	*76.2*	*78.9*	*77.8*	*175.8*		

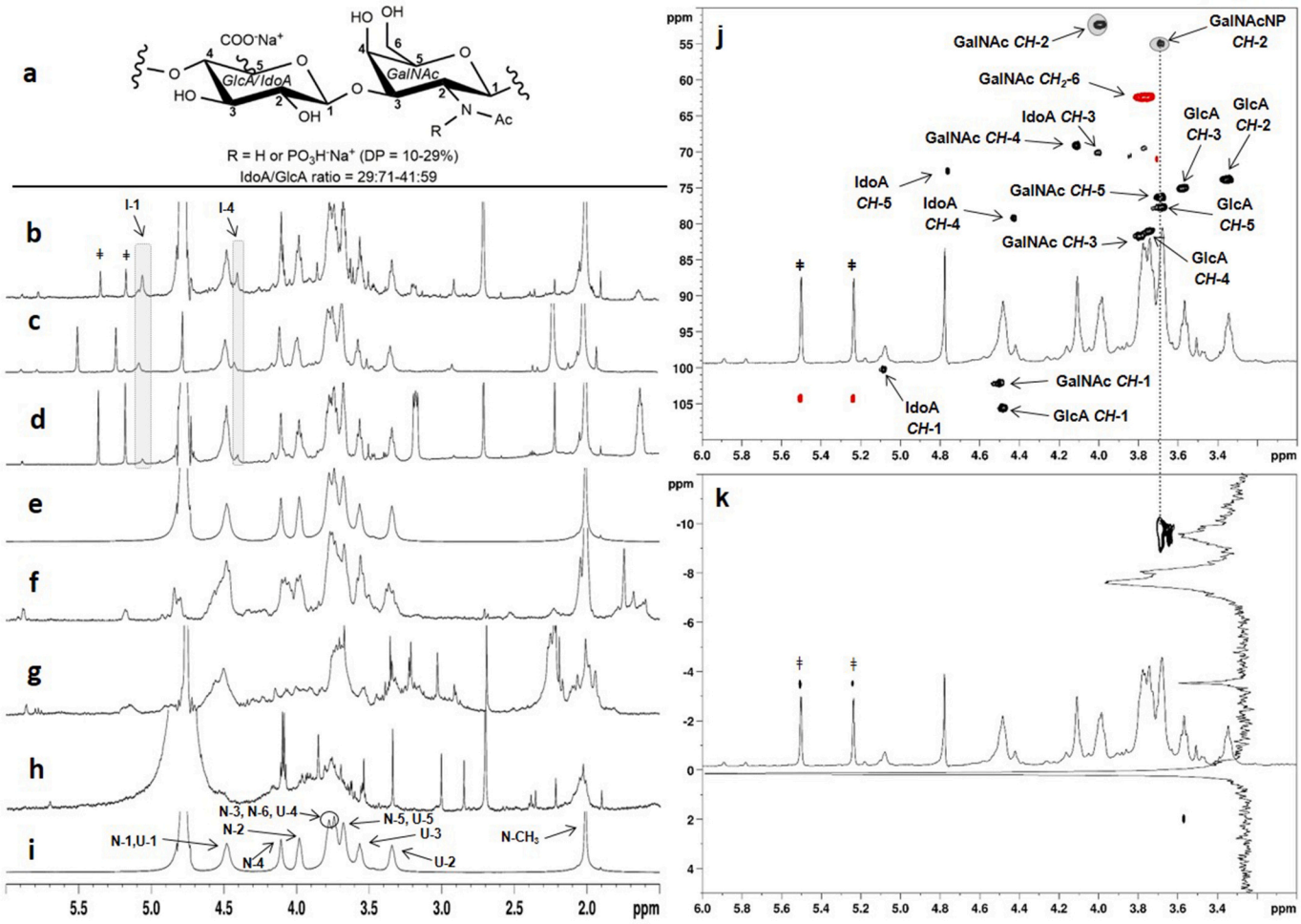

Fig. 4. (a) Structure of phosphorylated polysaccharides (CP-x and CP-xi; see Table 1 for details) semi-synthesized from derivative 2; (b-i) ^{1}H NMR spectra (600 MHz, 298 K, D_2O) of CP-xi (b), CP-X (c), CP-ix (d), CP-viii (e), CP-vii (f), CP-vi (g), CP-v (h) and CS-0 (i) (I = IdoA, N = GalNAc, NNP = GalNAcNP, U = GlcA; the grey stripes highlight the main differences among the spectra of CS-0 and CP-ix-xi); (j) superimposed ^{1}H NMR and ^{1}H,^{13}C-DEPT-HSQC 2D-NMR spectra (600 MHz, 298 K, D_2O) of CP-x (densities enclosed in grey circles were integrated for GalNAcNP *vs.* GalNAc relative amount estimation); (k) superimposed ^{1}H-, ^{31}P NMR and ^{1}H,^{31}P-HMBC 2D-NMR spectra (400 and 162 MHz, 298 K, D_2O) of CP-x (signals marked with ‡ symbol are relative to residual low molecular weight contaminants – *i.e.* PEP-K and/or derivatives thereof – as indicated by ^{1}H-DOSY NMR: see Fig. S9 in Supporting Information).

that could be identified by comparison with literature data (Pomin, 2014; Sudo et al., 2001) as an α-L-iduronic acid (IdoA) unit. Furthermore, the ^{1}H,^{13}C-DEPT-HSQC spectrum of CP-x and CP-xi revealed the presence of a low intense signal at $\delta_{H/C}$ 3.69/54.9 correlating with a ^{31}P signal at δ -9.4 in the ^{1}H,^{31}P-HMBC spectrum (Figs. 4k and S10-S11 in Supporting Information). This suggested the presence of a phosphate moiety linked to the nitrogen atom of some GalNAc units in CP-x and CP-xi polysaccharides. The relative amounts of these GalNAcNP residues with respect to unmodified GalNAc units could be estimated as 29 % and 10 % in CP-x and CP-xi, respectively, by relative integration of the GalNAc and GalNAcNP *CH*-2 signals volume in the ^{1}H,^{13}C-DEPT-HSQC spectrum.

The presence of unexpected GalNAcNP units in CP-x and CP-xi derivatives could be explained with a very low reactivity of the single unprotected hydroxyl at GalNAc *O*-4 position of starting polysaccharide 2. Indeed, it is very well known in synthetic carbohydrate chemistry that the *OH* at position 4 of acetamido-sugars is a very poor nucleophile (Crich & Dudkin, 2001). Its reactivity can be even lower than the acetamido group one (Liao & Auzanneau, 2005), that conversely is known to react readily with enol ester-type electrophiles (*e.g.* isopropenyl acetate) having chemical features resembling PEP-K structure (Suihko et al., 2001). The formation of IdoA units in CP-ix, CP-x and CP-xi was unexpected as well. It could be explained by an epimerization at the α-position of some of the GlcA methyl ester units of starting polysaccharide 2, plausibly activated by protic species present in the reaction mixture (PEP—K, TBAHS and the species afforded by their reaction; Domon et al., 2020). Indeed, the amount of IdoA units in CP derivatives was found to be directly dependent on PEP-K/TBAHS equivalents, with a marked increase from a 6 % value in CP-ix to 29 % and 41 % in CP-x and CP-xi, respectively (Table 2), as detected by relative integration of signals at δ 5.08 and 4.49–4.43 in the ^{1}H NMR spectra (see Fig. S12 in Supporting Information). Further investigations on the mechanism and the scope of such GlcA to IdoA epimerization are currently underway.

With respect to the structural characterization of the products obtained from chondroitin substrates 1 and 3, standard protocols employing H_3PO_4 or $POCl_3$ afforded highly heterogeneous products or negligible phosphorylation (Table 1, entries 12, 13, 15, 16 and Figs. S18-S19 in Supporting Information), while Ψ^{O}-based procedure gave no reaction at all (Table 1, entry 17). Conversely, by treating 3 with PEP-K and TBAHS in DMF at 100 °C, the targeted phosphorylation at GlcA *O*-2 site was clearly detected by ^{1}H,^{1}H-, ^{1}H,^{13}C- and ^{1}H,^{31}P-2D-NMR analysis of the obtained derivative CP-xviii (Table 2 and Figs. S16-S18 in Supporting Information), although a low DP (19 %) was estimated by ^{1}H,^{13}C-DEPT-HSQC integration. Furthermore, a trace amount (4 %) of phosphate groups attached at GalNAc *O*-6 site could be detected too. This could be ascribed to residual, unprotected GalNAc units along the

polysaccharide backbone of starting 3 and/or to the cleavage of some of the benzylidene rings protecting GaNAc units during the reaction. In both cases the phosphorylation of some GalNAc primary alcohols has been allowed. A much higher DP (80 %) was measured for GalNAc *O*-6 sites of derivative CP-xiv, obtained by treatment of precursor 1 with PEP-K and TBAHS (Table 1, entry 14). The $^{1}H,^{31}P$-HMBC spectrum of CP-xii (Fig. 5c) showed no further cross-peaks other than the one at $\delta_{H/P}$ 3.99/1.43, that was assigned to GalNAc *O*-6 phosphorylation. This suggested that no phosphate group insertion at GalNAc *O*-4 sites occurred, in agreement with the results described above for the phosphorylation of precursor 2. Nonetheless, the presence of a $^{1}H,^{13}C$-downfield shifted, non-anomeric signal at $\delta_{H/C}$ 4.76/77.1 in the $^{1}H,^{13}C$-DEPT-HSQC spectrum of CP-xiv (Fig. 5b) suggested the derivatization of some GalNAc units with a sulfate group at their *O*-4 site. This was confirmed by comparison with the chemical shift values reported for GalNAc4S *CH*-4 in A-type subunits of both natural (Mucci et al., 2000)

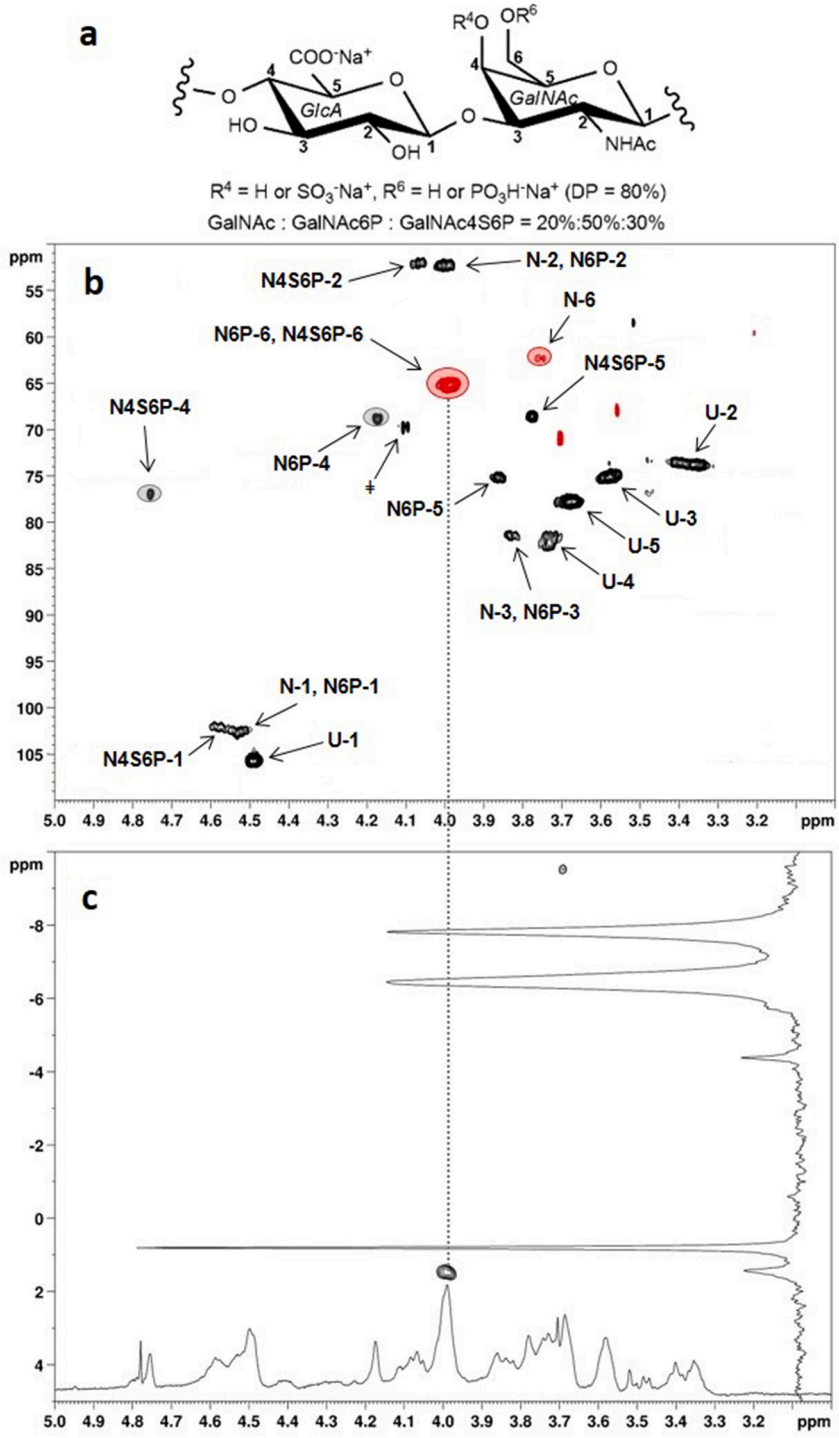

Fig. 5. (a) Structure of phosphorylated polysaccharide CP-xiv; (b) superimposed ^{1}H NMR and $^{1}H,^{13}C$-DEPT-HSQC 2D-NMR spectrum (600 MHz, 298 K, D_2O) of CP-xiv (N = GalNAc, N6P = GalNAc6P, N4S6P = GalNAc4S6P, U = GlcA; densities enclosed in red and grey circles were integrated for GalNAc:GalNAc6P:GalNAc4S6P relative amount estimation; signal marked with ‡ symbol is relative to a low molecular weight contaminant, as indicated by ^{1}H-DOSY NMR: see Fig. S14 in Supporting Information); (c) superimposed ^{1}H-, ^{31}P NMR and $^{1}H,^{31}P$-HMBC 2D-NMR spectra (400 and 162 MHz, 298 K, D_2O) of CP-xiv.

and semi-synthetic (Vessella, Marchetti, et al., 2021) CS polysaccharides. Noteworthy, a detailed study of COSY, TOCSY and ^{1}H,^{13}C-DEPT-HSQC spectra as well as the superimposition of the ^{1}H,^{13}C-heterocorrelated spectra of CP-xiv and semi-synthetic CS-A (Vessella, Marchetti, et al., 2021) (Figs. S16, S17 in Supporting Information) revealed that *O*-4 sulfation could be detected only in GalNAc units also carrying a phosphate group at *O*-6 position.

The presence of sulfate groups decorating CP-xiv was finally confirmed also by elemental analysis, giving a relative amount of sulfur atoms in the sample corresponding to a degree of sulfation (DS) value equal to 0.11, *i.e.* the presence of a sulfate group could be found in 11 % of the repeating units of CP-xiv polysaccharide. This DS value was in rough agreement with an estimation of a 20 %:50 %:30 % relative amount for GalNAc, GalNAc6P and GalNAc4S6P residues, respectively, as measured by relative integration of 6-*O*-phosphorylated *vs.* 6-*O*-underivatized GalNAc *CH*-6 and 4-*O*-sulfated *vs.* 4-*O*-underivatized GalNAc *CH*-4 couple of signals in the ^{1}H,^{13}C-DEPT-HSQC at $\delta_{H/C}$ 3.99/65.2, 3.78/62.4 and $\delta_{H/C}$ 4.76/77.1, 4.16/68.6, respectively.

The contemporary presence of both a phosphate and a sulfate group in some of GalNAc units in CP-xv is, to the best our knowledge, unprecedented in any GAG mimic. This unexpected structural feature could be explained with the mechanism proposed for phosphorylation with PEP-K/TBAHS reagents (Domon et al., 2020). Indeed, after phosphosulfophosphate (POSOP) has formed as active phosphate donor in the reaction mixture, its reaction with the primary alcohol group at GalNAc *O*-6 site allows the insertion of a phosphate moiety at this position and the contemporary release of phosphosulfate (POS), that can act not as phosphate but as sulfate donor on the proximal alcohol at *O*-4 position (Scheme 1). Such sulfation process was not detected on *O*-4 and/or *O*-6 sites of GalNAc units other than GalNAc4S6P, due to the competition of PEP-K for reaction on POS migrated far from its generation site to form POSOP again. Noteworthy, differently from CP-x and CP-xi obtained from 2, neither epimerization nor competitive *N*-phosphorylation processes were observed to occur in the reaction from 1 to CP-xiv.

4. Conclusions

In this work a microbial sourced chondroitin polysaccharide and three partially protected derivatives thereof have been subjected to phosphorylations under a set of different reaction conditions, in order to access for the first time the semi-synthesis of regioselectively phosphorylated GAG mimics. A detailed ^{1}H-, ^{13}C- and ^{31}P- one- and two-dimensional NMR analysis of the polysaccharides obtained after phosphorylation and, in case, subsequent cleavage of the protecting groups, revealed the higher versatility of a new, biomimetic phosphorylation method based on the combination of PEP-K and TBAHS, in comparison to standard reagents such as $POCl_3$ and H_3PO_4. In particular, reactions employing PEP-K or H_3PO_4 were both able to achieve the regioselective phosphorylation of the primary hydroxyl of GalNAc units on unprotected chondroitin, while only the former agent reacted on partially protected polysaccharide derivatives 1–3 in a controlled, regioselective fashion, affording a set of CP species with different derivatization patterns. Noteworthy, some of these products displayed an unexpected chemical structure, with the combined insertion of a sulfate and a phosphate group at GalNAc *O*-4 and *O*-6 positions, respectively, or with a GlcA to IdoA epimerization.

Encouraged by the here presented results, the scope of the regioselective phosphorylation with PEP-K/TBAHS on polysaccharides other than microbial sourced chondroitin is currently under investigation, in order to enlarge the set of phosphorylated GAG mimics and then assay them for their biological activities in comparison with native sulfated GAGs. An enlargement of the screening of regioselective phosphorylation procedures applicable to polysaccharides is currently underway too.

CRediT authorship contribution statement

Fabiana Esposito: Conceptualization, Data curation, Investigation, Writing – review & editing. **Serena Traboni:** Conceptualization, Writing – review & editing. **Alfonso Iadonisi:** Conceptualization, Writing – review & editing. **Emiliano Bedini:** Conceptualization, Data curation, Methodology, Supervision, Validation, Writing – original draft.

Declaration of competing interest

The authors declare that they have no known competing financial interests or personal relationships that could have appeared to influence the work reported in this paper.

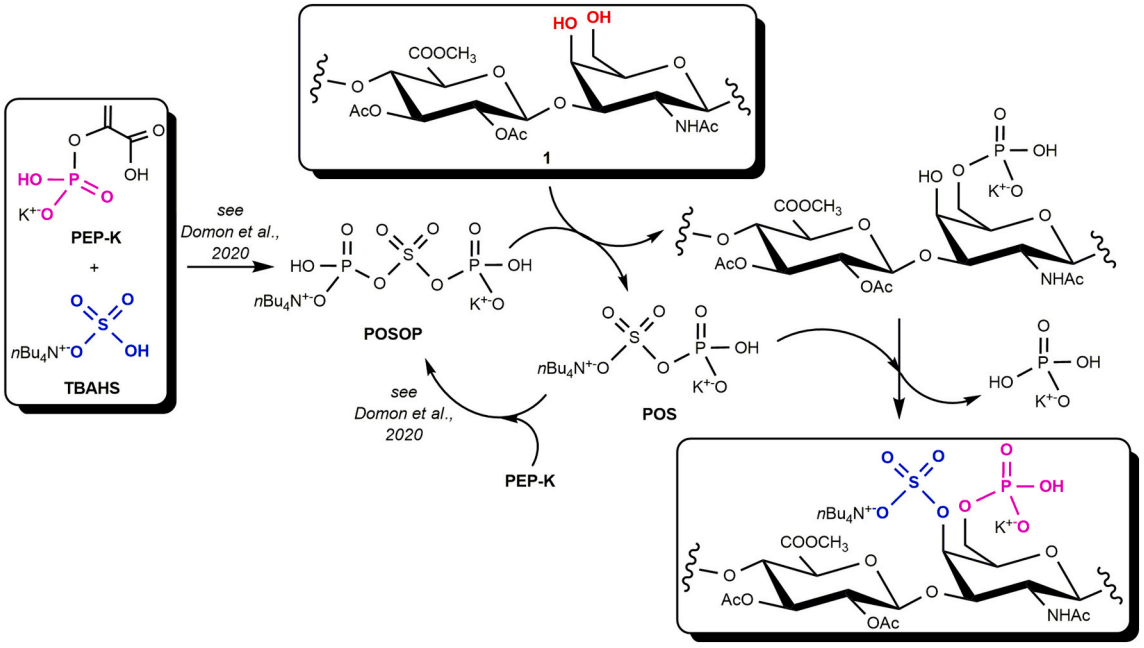

Scheme 1. Proposed mechanism for the obtainment of GalNAc4S6P units in CP-xiv by treating 1 with PEP-K/TBAHS

Data availability

Data will be made available on request.

Acknowledgments

This research did not receive any specific grant from funding agencies in the public, commercial, or not-for-profit sectors.

Appendix A. Supplementary data

Supplementary data to this article can be found online at https://doi.org/10.1016/j.carbpol.2023.121517.

References

Afosah, D. K., & Al-Rohani, R. A. (2020). Sulfated non-saccharide glycosaminoglycan mimetics as novel drug discovery platform for various pathologies. *Current Medicinal Chemistry, 27*, 3412–3447.

Alfieri, M. L., Panzella, L., Duarte, B., Gonçalves-Monteiro, S., Marques, F., Morato, M., … Napolitano, A. (2021). Sulfated oligomers of tyrosol: Toward a new class of bioinspired nonsaccharidic anticoagulants. *Biomacromolecules, 22*, 399–409.

Arlov, Ø., Rütsche, D., Korayem, M. A., Öztürk, E., & Zenobi-Wong, M. (2021). Engineered sulfated polysaccharides for biomedical applications. *Advanced Functional Materials, 2010732*.

Badri, A., Williams, A., Awofiranye, A., Datta, P., Xia, K., He, W., … Koffas, M. A. G. (2021). Complete biosynthesis of a sulfated chondroitin in *Escherichia coli*. *Nature Communications, 12*, 1389.

Bedini, E., De Castro, C., De Rosa, M., Di Nola, A., Iadonisi, A., Restaino, O. F., … Parrilli, M. (2011). A microbiological-chemical strategy to produce chondroitin sulfate A,C. *Angewandte Chemie International Edition, 50*, 6160–6163.

Bedini, E., Laezza, A., Parrilli, M., & Iadonisi, A. (2017). A review of chemical methods for the selective sulfation and desulfation of polysaccharides. *Carbohydrate Polymers, 174*, 1224–1239.

Bojarski, K. K., Becher, J., Riemer, T., Lemmnitzer, K., Möller, S., Schiller, J., … Samsonov, S. A. (2019). Synthesis and in silico characterization of artificially phosphorylated glycosaminoglycans. *Journal of Molecular Structure, 1197*, 401–416.

Cimini, D., Bedini, E., & Schiraldi, C. (2023). Biotechnological advances in the synthesis of modified chondroitin towards novel biomedical applications. *Biotechnology Advances, 67*, Article 108185.

Cimini, D., Restaino, O. F., & Schiraldi, C. (2018). Microbial production and metabolic engineering of chondroitin and chondroitin sulfate. *Emerging Topics in Life Sciences, 2*, 349–361.

Coleman, R. J., Lawrie, G., Lambert, L. K., Whittaker, M., Jack, K. S., & Grøndahl, L. (2011). Phosphorylation of alginate: Synthesis, characterization, and evaluation of *in vitro* mineralization capacity. *Biomacromolecules, 12*, 889–897.

Collin, E. C., Carroll, O., Kilcoyne, M., Peroglio, M., See, E., Hendig, D., … Pandit, A. (2017). Ageing affects chondroitin sulfates and their synthetic enzymes in the intervertebral disc. *Signal Transduction and Targeted Therapy, 2*, 17049.

Crich, D., & Dudkin, V. (2001). Why are the hydroxy groups of partially protected *N*-acetylglucosamine derivatives such poor glycosyl acceptors, and what can be done about it? A comparative study of the reactivity of *N*-acetyl-, *N*-phthalimido-, and 2-azido-2-deoxy-glucosamine derivatives in glycosylation. 2-Picolinyl ethers as reactivity-enhancing replacements for benzyl ethers. *Journal of the American Chemical Society, 123*, 6819–6825.

Domon, K., Puripat, M., Fujiyoshi, K., Hatanaka, M., Kawashima, S. A., Yamatsugu, K., & Kanai, M. (2020). Catalytic chemoselective *O*-phosphorylation of alcohols. *ACS Central Science, 6*, 283–292.

Gottschalk, J., & Elling, L. (2021). Current state on the enzymatic synthesis of glycosaminoglycans. *Current Opinion in Structural Biology, 61*, 71–80.

Guerrini, M., Beccati, D., Shriver, Z., Naggi, A., Viswanathan, K., Bisio, A., … Sasisekharan, R. (2008). Oversulfated chondroitin sulfate is a contaminant in heparin associated with adverse clinical events. *Nature Biotechnology, 26*, 669–675.

Guerrini, M., Naggi, A., Guglieri, S., Santarsiero, R., & Torri, G. (2005). Complex glycosaminoglycans: Profiling substitution patterns by two-dimensional nuclear magnetic resonance spectroscopy. *Analytical Biochemistry, 337*, 35–47.

Han, X., Sanderson, P., Nesheiwat, S., Lin, L., Yu, Y., Zhang, F., … Linhardt, R. J. (2020). Structural analysis of urinary glycosaminoglycans from healthy human subjects. *Glycobiology, 30*, 143–151.

Illy, N., Fache, M., Ménard, R., Negrell, C., Caillol, S., & David, G. (2015). Phosphorylation of bio-based compounds: The state of the art. *Polymer Chemistry, 6*, 6257–6291.

Khaybrakhmanova, E. A., Kozyrev, S. V., Tyumkina, T. V., & Ponedel'kina, I. Y. (2022). Phosphorylation of hyaluronic acid. *Chemical Proceedings, 12*, 39.

Knouse, K. W., Flood, D. T., Vantourout, J. C., Schmidt, M. A., Mcdonald, I. M., Eastgate, M. D., & Baran, P. S. (2021). Nature chose phosphates and chemists should too: How emerging P(V) methods can augment existing strategies. *ACS Central Science, 7*, 1473–1485.

Laffargue, T., Moulis, C., & Remaud-Siméon, M. (2023). Phosphorylated polysaccharides: Applications, natural abundance, and new-to-nature structures generated by chemical and enzymatic functionalization. *Biotechnology Advances, 65*, Article 108140.

Liao, L., & Auzanneau, F.-I. (2005). The amide group in *N*-acetylglucosamine glycosyl acceptors affects glycosylation outcome. *The Journal of Organic Chemistry, 70*, 6265–6273.

Lin, H., Leman, L. J., & Krishnamurthy, R. (2022). One-pot chemical pyro- and tri-phosphorylation of peptides by using diamidophosphate in water. *Chemical Science, 13*, 13741–13747.

Liu, Q., Chen, G., & Chen, H. (2019). Chemical synthesis of glycosaminoglycan-mimetic polymers. *Polymer Chemistry, 10*, 164–171.

Lowman, D., Ensley, H., & Williams, D. (1998). Identification of phosphate substitution sites by NMR spectroscopy in a water-soluble phosphorylated (1→3)-β-D-glucan. *Carbohydrate Research, 306*, 559–562.

Mende, M., Bednarek, C., Wawryszyn, M., Sauter, P., Biskup, M. B., Schepers, U., & Bräse, S. (2016). Chemical synthesis of glycosaminoglycans. *Chemical Reviews, 116*, 8193–8255.

Morla, S., Ravikumar, O., O'Hara, C., Boothello, R., Vera, A., Abdelfadiel, E. I., … Desai, U. R. (2023). Designing synthetic, sulfated glycosaminoglycan mimetics that are orally bioavailable and exhibiting *in vivo* anticancer activity. *Journal of Medicinal Chemistry, 66*, 1321–1338.

Mucci, A., Schenetti, L., & Volpi, N. (2000). ^{1}H and ^{13}C nuclear magnetic resonance identification and characterization of components of chondroitin sulfates of various origin. *Carbohydrate Polymers, 41*, 37–45.

Nie, C., Pouyan, P., Lauster, D., Trimpert, J., Kerkhoff, Y., Szekeres, G. P., … Haag, R. (2021). Polysulfates block SARS-CoV-2 uptake through electrostatic interactions. *Angewandte Chemie International Edition, 60*, 15870–15878.

Niu, S., Wang, J., Zhao, B., Zhao, M., Nie, M., Wang, X., Yao, J., & Zhang, J. (2013). Regioselective synthesis and antioxidant activities of phosphorylated guar gum. *International Journal of Biological Macromolecules, 62*, 741–747.

Ociepa, M., Knouse, K. W., He, D., Vantourout, J. C., Flood, D. T., Padial, N. M., … Baran, P. S. (2021). Mild and chemoselective phosphorylation of alcohols using a Ψ-reagent. *Organic Letters, 23*, 9337–9342.

Perez, S., Makshakova, O., Angulo, J., Bedini, E., Bisio, A., de Paz Carrera, J. L., … Ricard Blum, S. (2023). Glycosaminoglycans: What remains to be deciphered? *Journal of the American Chemical Society Au, 3*, 628–656.

Pomin, V. H. (2014). NMR chemical shifts in structural biology of glycosaminoglycans. *Analytical Chemistry, 86*, 65–94.

Pomin, V. H. (2015). A dilemma in the glycosaminoglycan-based therapy: Synthetic or naturally unique molecules? *Medical Research Reviews, 35*, 1195–1219.

Restaino, O. F., Finamore, R., Diana, P., Marseglia, M., Vitiello, M., Casillo, A., … Schiraldi, C. (2017). A multi-analytical approach to better assess the keratan sulfate contamination in animal origin chondroitin sulfate. *Analytica Chimica Acta, 958*, 59–70.

Schmieder, P., Nitschke, F., Steup, M., Mallow, K., & Specker, E. (2013). Determination of glucan phosphorylation using heteronuclear ^{1}H,^{13}C double and ^{1}H,^{13}C,^{31}P triple-resonance NMR spectra. *Magnetic Resonance in Chemistry, 51*, 655–661.

Soares da Costa, D., Reis, R. L., & Pashkuleva, I. (2017). Sulfation of glycosaminoglycans and its implications in human health and disorders. *Annual Review of Biomedical Engineering, 19*, 1–26.

Sudo, M., Sato, K., Chaidedgumjorn, A., Toyoda, H., Toida, T., & Imanari, T. (2001). ^{1}H nuclear magnetic resonance spectroscopic analysis for determination of glucuronic and iduronic acids in dermatan sulfate, heparin, and heparan sulfate. *Analytical Biochemistry, 297*, 42–51.

Suihko, M., Ahlgrén, M., Aulaskari, P., & Rouvinen, J. (2001). Improved synthesis and characterization of 1,3,4,6-tetra-*O*-acetyl-2-(*N*-acetylacetamido)-2-deoxy-β-D-glucopyranose. *Carbohydrate Research, 334*, 337–341.

Tyrikos-Ergas, T., Sletten, E. T., Huang, J.-Y., Seeberger, P. H., & Delbianco, M. (2022). On resin synthesis of sulfated oligosaccharides. *Chemical Science, 13*, 2115–2120.

Varghese, M., Haque, F., Lu, W., & Grinstaff, M. W. (2022). Synthesis and characterization of regioselectively functionalized mono-sulfated and -phosphorylated anionic poly-amido-saccharides. *Biomacromolecules, 23*, 2075–2088.

Vessella, G., Marchetti, R., Del Prete, A., Traboni, S., Iadonisi, A., Schiraldi, C., Silipo, A., & Bedini, E. (2021). Semisynthetic isomers of fucosylated chondroitin sulfate polysaccharides with fucosyl branches at a non-natural site. *Biomacromolecules, 22*, 5151–5161.

Vessella, G., Traboni, S., Cimini, D., Iadonisi, A., Schiraldi, C., & Bedini, E. (2019). Development of semisynthetic, regioselective pathways for accessing the missing sulfation patterns of chondroitin sulfate. *Biomacromolecules, 20*, 3021–3030.

Vessella, G., Traboni, S., Pirozzi, A. V. A., Laezza, A., Iadonisi, A., Schiraldi, C., & Bedini, E. (2019). A study for the access to a semi-synthetic regioisomer of natural fucosylated chondroitin sulfate with fucosyl branches on *N*-acetyl-galactosamine units. *Marine Drugs, 17*, 655.

Vessella, G., Vázquez, J. A., Valcárcel, J., Lagartera, L., Monterrey, D. T., Bastida, A., … Revuelta, J. (2021). Deciphering structural determinants in chondroitin sulfate binding to FGF-2: Paving the way to enhanced predictability of their biological functions. *Polymers, 13*, 313.

Volpi, N., Galeotti, F., Maccari, F., Capitani, F., & Mantovani, V. (2021). Structural definition of terrestrial chondroitin sulfate of various origin and repeatability of the production process. *Journal of Pharmaceutical and Biomedical Analysis, 195*, Article 113826.

Wang, N., Kong, Y., Li, J., Hu, Y., Li, X., Jiang, S., & Dong, C. (2022). Synthesis and application of phosphorylated saccharides in researching carbohydrate-based drugs. *Bioorganic & Medicinal Chemistry, 68*, Article 116806.

Zeng, K., Groth, T., & Zhang, K. (2019). Recent advances in artificially sulfated polysaccharides for applications in cell growth and differentiation, drug delivery, and tissue engineering. *ChemBioChem, 20*, 737–746.

Zhang, X., Lin, L., Huang, H., & Linhardt, R. J. (2020). Chemoenzymatic synthesis of glycosaminoglycans. *Accounts of Chemical Research, 53*, 335–346.

Zhou, S., & Huang, G. (2021). Preparation, structure and activity of polysaccharide phosphate esters. *Biomedicine & Pharmacotherapy, 144*, Article 112332.